THE JOURNAL OF PHYSICAL CHEMISTRY B

Article

pubs.acs.org/JPCB

Effect of Solvent Dielectric Constant and Acidity on the OH Vibration Frequency in Hydrogen-Bonded Complexes of Fluorinated Ethanols

Dina Pines,[†] Sharon Keinan,[†] Philip M. Kiefer,[‡] James T. Hynes,*[,‡,§] and Ehud Pines*[,†]

[†]Department of Chemistry, Ben-Gurion University of the Negev, P.O. Box 653, Beer-Sheva, 84105, Israel

[‡]Department of Chemistry and Biochemistry, University of Colorado, Boulder, Colorado 80309-0215, United States

[§]Chemistry Department, École Normale Supérieure, UMR ENS-CNRS-UPMC 8640, 24 rue Lhomond, 75005 Paris, France

ABSTRACT: Infrared spectroscopy measurements were used to characterize the OH stretching vibrations in a series of similarly structured fluoroethanols, RCH_2OH (R = CH_3, CH_2F, CHF_2, CF_3), a series which exhibits a systematic increase in the molecule acidity with increasing number of F atoms. This study, which expands our earlier efforts, was carried out in non-hydrogen-bonding solvents comprising molecules with and without a permanent dipole moment, with the former solvents being classified as polar solvents and the latter designated as nonpolar. The hydrogen bond interaction in donor−acceptor complexes formed in solution between the fluorinated ethanol H-donors and the H-acceptor base DMSO was investigated in relation to the solvent dielectric and to the differences ΔPA of the gas phase proton affinities (PAs) of the conjugate base of the fluorinated alcohols and DMSO. We have observed that ν_{OH} decreases as the acidity of the alcohol increases (ΔPA decreases) and that ν_{OH} varies inversely with ε, exhibiting different slopes for nonpolar and polar solvents. These $1/\varepsilon$ slopes tend to vary linearly with ΔPA, increasing with increasing acidity. These experimental findings, including the ΔPA trends, are described with our recently published two-state Valence Bond-based theory for acid−base H-bonded complexes. Lastly, the correlation of the alcohol's conjugate base PAs with Taft σ^* values of the fluorinated ethyl groups $CH_nF_{3-n}CH_2-$ provides a connection of the inductive effects for these groups with the acidity parameter ΔPA associated with the H-bonded complexes.

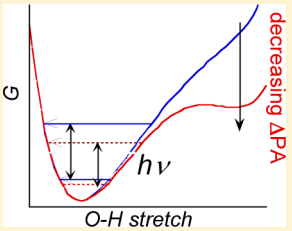

1. INTRODUCTION

Hydrogen (H)-bonding interactions greatly affect the structure and reactivity of countless chemical and biochemical systems.[1−5] In solution, H-bonds are an important part of solute−solvent interactions and represent a major component of the reaction coordinate for proton transfer between acids and bases, both in ground and electronically excited states of the reactants.[6−10]

In recent publications, we have developed an experimental approach and an accompanying theory for the proton stretch vibrational frequency ν_{AH} in an H-bonded complex AH···B and its variation with $1/\varepsilon$, the inverse of the solvent dielectric constant; the experimental observations and theoretical descriptions were in good accord.[11,12] In particular, we have applied Kamlet−Taft empirical solvent polarity parameters for identifying the origins of the solvent effect on a carefully selected group of H-bonded complexes in non-H-bonding solvents and used them as indicators for the underlying physical quantities which determine the observed experimental vibrational frequency behavior.

To enable this identification, we used well-characterized families of H-bonded complexes that indeed have allowed a productive two-pronged experimental and theoretical study. We ensured that the structure of the H-bonded complexes is little varied by either the solvent or the strength of the H-bonding interaction. In addition, our study was limited to molecules where steric effects are minimal and to H-bonded complexes belonging to the OH···O type complex family.

Specifically, we have focused experimentally on the OH frequency in 1:1 complexes of aromatic alcohols and ethanol H-bonded to DMSO, and were able to construct a general theory for this frequency and its solvent dependence in terms of basic physical quantities.[11,12] These included the size of the H-bond complex, the dipole moments of the neutral and proton-transferred H-bond complexes, and the difference in acidity between the acid proton donor and the base proton acceptor, measured by an appropriate difference in proton affinities. We were also able for the first time to experimentally establish and theoretically rationalize a $1/\varepsilon$ dependence for the H-bond−solvent interaction, and to distinguish by this correlation between solvents whose molecules do (polar) or do not (nonpolar) have a permanent dipole moment.

In the present contribution, we expand our two-pronged approach. In particular, here we use a selective family of H-bonded complexes which share a similar overall structure and similar chemical reactivity—but with, e.g., varying acidity due to varying substitution—in order to further examine the role of acidity in determining the magnitude of ν_{OH} as a readily accessed experimental variable of the H-bonded complex.

Alcohols of the type RCH_2OH (ethanol (EtOH), R = CH_3, monofluoroethanol (MFE), R = CH_2F, difluoroethanol (DFE),

Special Issue: Branka M. Ladanyi Festschrift

Received: September 30, 2014
Revised: November 23, 2014
Published: November 24, 2014

ACS Publications © 2014 American Chemical Society

R = CHF_2, trifluoroethanol (TFE), R = CF_3) form an excellent series of model aliphatic OH acids, in which the acidity is systematically varied without changing the proton donor group and without appreciably affecting the H-bond donor's general structure and the size.[13,14] We first examine the spectral features of the OH absorption of the uncomplexed ROH acids in nonpolar and polar solvents, and then compare them with the OH absorption of their respective H-bonded complexes when complexed with the base DMSO in various solvents. Lastly, the correlation of the alcohol's conjugate base PAs with Taft σ^* values[15] of the fluorinated ethyl groups $CH_nF_{3-n}CH_2-$ provides a connection of the inductive effects for these groups with the acidity parameter ΔPA associated with the H-bonded complexes.

We then analyze the solvent effect on ν_{OH}(complex) of this family of alcohols/acids complexed with DMSO. The solvents employed dielectric constants ranging from 1.8 to 10.3[16] and were chosen according to criteria similar to those applied in our previous publications.[11,12] Specifically, these aprotic solvents do not specifically interact with the ethanols' O−H moiety. They exhibit a negligible basicity, as judged by their very small Kamlet−Taft basicity scale value (β)[17] which was less or equal to 0.1. These values are much smaller than the basicity 0.76 of DMSO, the complexing base.[18] The Kamlet−Taft acidity value (α)[19] for the solvents is zero in general with the exceptions of chloroform and dichloromethane (DCM), which have small acidity values of 0.2 and 0.13, respectively.[18]

The remainder of this paper is organized as follows. The experimental details are given in section 2 and the experimental findings are described in section 3, both for measurements done in neat solvents where the DMSO base is absent and the acids interact solely with the solvents and for the acid−DMSO complexes in these solvents. In section 4, we first focus on the interpretation of the slopes of the frequency shift $\Delta\nu_{OH}$ versus the solvent inverse dielectric constant, and we then turn to those features primarily related to the effect of the acidity of the fluorinated ethanol moiety in the H-bonded complex. We also relate aspects of this behavior to the well-known Taft σ^* parameter. Finally, we summarize and conclude our discussion in section 5.

2. EXPERIMENTAL SECTION

Fourier transform infrared (FTIR) spectra were recorded by using a Jasco FT/IR-6300 spectrometer with a 1−2 cm^{-1} wavenumber resolution in the 700−4000 cm^{-1} region. All measurements were performed at room temperature (22 ± 1 °C) in CaF_2 cells. Both 50 μm and 1 mm path-length cells were used with no detectable differences.

Fluoroethanols were from Sigma-Aldrich (>99%). All solvents were purchased in anhydrous form with less than 50 ppm water content and kept in sealed bottles under nitrogen. The concentrations of the various ethanols ranged from 0.01 to 0.02 M with DMSO concentrations ranging from 0.01 to 0.05 M for all solvents.

To ensure that no oligomers had been formed in solution, the IR spectra of the alcohols were taken before adding the complexing-base DMSO and matched with the IR spectra of the alcohols at high dilution (0.005 M), to ensure the constancy of the spectral shape of the "free" OH absorption under the conditions of higher alcohol concentrations and partial complexation with DMSO. In addition, the IR spectra of the DMSO-complexed ethanols were checked as a function of the DMSO concentration for constancy and for verifying that only two OH stretch IR bands appear in the spectra: a narrow absorption band of the uncomplexed OH and a much wider red-shifted absorption band of the H-bonded OH.

The maximum absorption ν_{OH} was obtained by fitting the top of the broad absorption spectra of the DMSO-complexed ethanols with a Gaussian function and then using the maximum of the Gaussian function as the ν_{OH} value of the H-bonded complexes. A similar fitting procedure was also applied to the much narrower absorption spectra of the uncomplexed OH in order to achieve standardization of our method of spectral analysis. The numeric ν_{OH} values that were obtained by the Gaussian fits differed by no more than 1−2 cm^{-1} from the ν_{OH} values taken directly from the measured IR spectra.

3. RESULTS

3.1. Uncomplexed Alcohols in Polar and Nonpolar Solvents. The infrared (IR) spectra of aliphatic alcohols and phenols in non-H-bonding solvents share an intense, relatively narrow and symmetric absorption band at about 3600 cm^{-1}, which corresponds to the absorption of the OH stretch vibration ν_{OH}. Typical IR absorption spectra of difluoroethanol (CHF_2CH_2OH) in four representative solvents are shown in Figure 1.

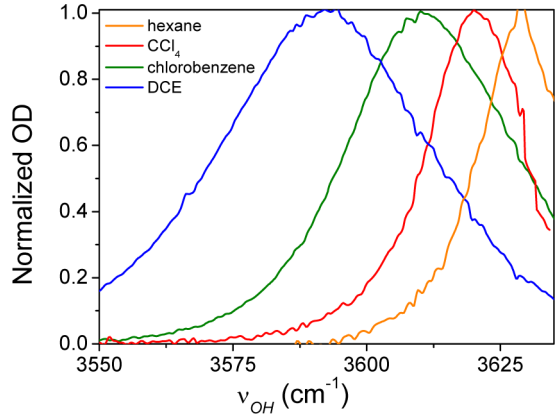

Figure 1. Normalized IR absorption spectra of ν_{OH} of difluoroethanol in several non-H-bonding solvents (nos. 2, 4, 7, and 11 in Table 1) representing the polar and nonpolar solvent groups. The full set of the measured spectra is not shown because of graphic crowding. The frequencies of the maximum absorption ν_{OH} are summarized in Table 1. The full width at half-maximum (fwhm) values of the IR absorption bands are 15, 19, 35, and 45 cm^{-1} for ethanol, monofluoroethanol (MFE), difluoroethanol (DFE), and trifluoroethanol (TFE), respectively.

A gradual linear increase in both the width of the absorption spectra and the red-shift in the maximum of ν_{OH} was clearly visible with an increase in solvent polarity, as measured by the static solvent dielectric constant ε (Table 1). The frequencies of the maximum absorption ν_{OH} are summarized in Table 1 but excluding perfluoroheptane for ethanol and monofluoroethanol because of the low solubility of these alcohols in perfluoroheptane and consequently poor S/N of their IR spectra.

The solvent-induced red-shifts listed in Table 1 are substantial, amounting to about 60 and 55 cm^{-1} for DFE and TFE, respectively, when moving from perfluoroheptane to dichloroethane solvent.

As we have previously demonstrated,[12] the "free" (non-complexed) absorption of the OH oscillator may be used to

dx.doi.org/10.1021/jp509914w | J. Phys. Chem. B 2015, 119, 9278−9286

Table 1. Refractive Index n, n^2, the Static Dielectric Constant ε,[16] the Frequency of the Maximum Absorption ν_{OH} for the Solvents Used in this Study, and the Number of Fluorine Atoms n_F

no.		n	n^2	ε	ν_{OH}, ethanol, $n_F = 0$	ν_{OH}, MFE, $n_F = 1$	ν_{OH}, DFE, $n_F = 2$	ν_{OH}, TFE, $n_F = 3$
				Nonpolar Solvents				
1	perfluoroheptane	1.258^{20}	1.58	1.765^{20}			3647	3647
2	hexane	1.375	1.89	1.88	3643	3630	3630.5	3630
3	cyclohexane	1.426	2.01	2.01	3638	3624	3625.5	3625
4	CCl_4[a]	1.460	2.13	2.23	3634	3621	3620.5	3620
5	TCE[b]	1.504	2.23	2.27	3630	3619	3618	3617
6	CS_2[c]	1.630	2.65	2.64	3619	3607	3605	3604
				Polar Solvents				
7	chloroform	1.446	2.09	4.81	3621	3614	3613.5	3611
8	chlorobenzene	1.525	2.32	5.62	3614	3607	3598	3594
9	DCM[d]	1.424	2.03	8.93	3615	3609	3604.5	3596
10	1,2-dichlorobenzene	1.551	2.41	9.90	3618			3598.5
11	DCE[e]	1.445	2.09	10.37	3607	3599	3592.5	3587

[a]Tetrachloromethane. [b]Tetrachloroethene. [c]Carbondisulfide. [d]Dichloromethane. [e]1,2-Dichloroethane.

differentiate polar and nonpolar solvents. Nonpolar solvents are those for which the dielectric constant originates from a purely electronic response. The molecules of these solvents have no permanent dipole moment, and the solvent dielectric constant ε is almost identical to n^2, the square of the solvent refractive index (cf. Table 1). For polar solvents, whose molecules have a permanent dipole moment, an additional and often very significant contribution to the dielectric response ε originates from spatial rearrangement, especially reorientation, of the molecule's permanent dipole moment: this is an extremely slow process compared to electronic rearrangement.

Figure 2 highlights a clear distinction between the effect of nonpolar and polar solvents on ν_{OH} ("free"). A linear correlation is evident between the ν_{OH} ("free") of fluorinated alcohols and $1/n^2$ in nonpolar solvents and perfluorinated heptane, solvents 1−6 in Table 1. However, for the polar solvents in Table 1 (solvents 7−11), no such correlation with $1/n^2$ is observed: all the data points seem to be randomly distributed *below* the correlation line of the nonpolar solvents, i.e., a larger red-shift. This lack of correlation is not surprising, since, for the polar solvents, the dielectric constant is considerably larger than n^2 (Table 1) and the solvent effect on ν_{OH} depends in part on solvent reorientation modes which are subject to dielectric loss. Thus, nonpolar solvents are important for demonstrating the effect of nonspecific dielectric solvation not only because they lack specific H-bonding interactions but also—in contrast to polar solvents—because their dielectric response is practically immediate on the time scale of the OH vibration and the hydrogenic motion. We do not pursue further the distinction between nonpolar and polar solvation effects on the noncomplexed alcohol ν_{OH}, since, as was detailed in ref 12, isolation of solvent effects requires the study of appropriate H-bonded complexes.

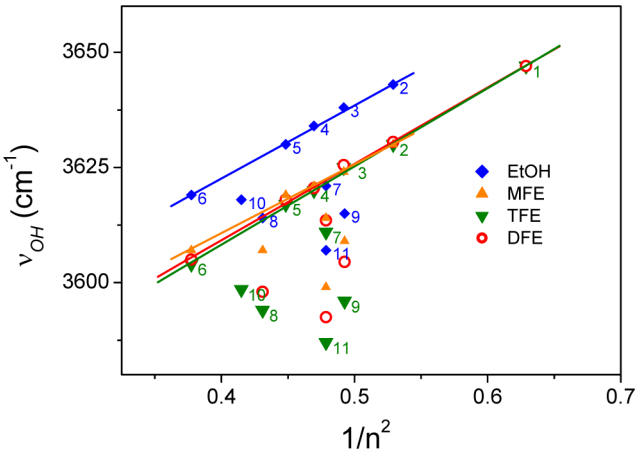

Figure 2. Plot of ν_{OH} of noncomplexed fluoroethanols versus the inverse of the square of the solvent index of refraction $1/n^2$ for solvents listed according to their respective numbers in Table 1. The apparent linear correlation between ν_{OH} and $1/n^2$ for the nonpolar solvents (nos. 1−6) has a slope of 158 cm^{-1} for ethanol (R = 0.999), a slope of 150 cm^{-1} for monofluoroethanol (R = 0.998), a slope of 165 cm^{-1} for difluoroethanol (R = 0.999), and a slope of 169 cm^{-1} for trifluoroethanol (R = 0.999). The polar solvents (nos. 7−11) do not exhibit this linear correlation.

A final observation based on Figure 2 is that ethanol does not group together with the three fluoroethanols, which among themselves exhibit similar absorption frequencies and a similar sensitivity to $1/n^2$. The origin of this "gap" is in the isolated molecules: the same spectral grouping is observed for the gas phase −OH IR absorption. For ethanol, ν_{OH} is 3676 cm^{-1}, while the frequencies for the three fluoroethanols are red-shifted and lumped together: monofluoroethanol, 3660 cm^{-1}; difluoroethanol, 3659 cm^{-1}; trifluoroethanol, 3658 cm^{-1}.[13,14,21]

We will now see that the H-bonded complexes of the four ethanols exhibit a different case than the "free" ethanols and are well-modeled by our two-state Valence Bond-based theory which was developed for H-bonded complexes. As demonstrated below, for H-bonded complexes, the theory suggests and experiment corroborates that ν_{OH}(complexed) correlates well with $1/\varepsilon$ for both nonpolar and polar solvents with different correlation slopes which are directly accounted for by the theory.

3.2. H-Bonded Complexes of Fluoroethanols with DMSO in Polar and Nonpolar Solvents. In order to experimentally investigate the effect of nonspecific polar interactions and the influence of varying acidity on the OH frequency ν_{OH}, and to enable direct comparison with theory, we have measured the OH absorption of complexes of fluoroethanols (including ethanol) involving an H-bond to the base dimethyl sulfoxide (DMSO) in solvents 2−11 (see Table 1). The frequencies of the maximum absorption ν_{OH} are summarized in Table 2. Increasing the number of fluorine atoms attached to the ethanol molecule's alkyl group acts to

dx.doi.org/10.1021/jp509914w | J. Phys. Chem. B 2015, 119, 9278−9286

Table 2. Frequency of the Maximum Absorption ν_{OH} for the Substituted Ethanol−DMSO H-Bonded Complexes in the Solvents Used in This Study

no.		ν_{OH}, EtOH	ν_{OH}, MFE	ν_{OH}, DFE	ν_{OH}, TFE
		Nonpolar Solvents			
1	perfluoroheptane			3386	3345
2	hexane	3445	3405	3380	3334
3	cyclohexane	3440	3399	3370	3326
4	CCl_4	3433	3392	3360	3316
5	TCE	3432	3391	3358	3314
6	CS_2	3430	3384	3350	3304
		Polar Solvents			
7	chloroform	3424	3378	3336	3288
8	chlorobenzene	3423	3376	3333	3285
9	DCM	3420	3371	3327	3276
11	DCE	3420	3370	3326	3275

systematically increase the donating capacity of the parent proton donor molecule. This increase via fluorosubstitution at the beta carbon atom causes a variation in the H-bond strength over a wide acidity range without changing the atoms directly involved in the H-bond (O−H···O).

The formation of H-bonded complexes was accompanied by reduced monomeric O−H absorption concomitant with the appearance of the red-shifted complex band. The location of the spectral maxima for the DMSO-bonded complexes in different solvents depends on both the number of the fluorine atoms n_F and the solvent dielectric constant. When the OH group of the fluoroethanols is involved in H-bond interaction, the absorption of the OH bond is red-shifted from its uncomplexed value (larger magnitude of $\Delta\nu_{OH}$) and becomes very broad. Typical examples for the IR spectra of the H-bonded complexes of the four ethanols in CCl_4 are shown in Figure 3.

The experimental data collected for the H-bonded complexes of the four ethanols is summarized in Table 2. (excluding perfluoroheptane for ethanol and monofluoroethanol, because of their low solubility in perfluoroheptane). The division into nonpolar and polar solvents is identical to that in Table 1 for the uncomplexed ethanols. We classify perfluoroheptane as a nonpolar solvent, although ε is slightly larger than n^2 because it correlates according to n^2; see Figure 2.

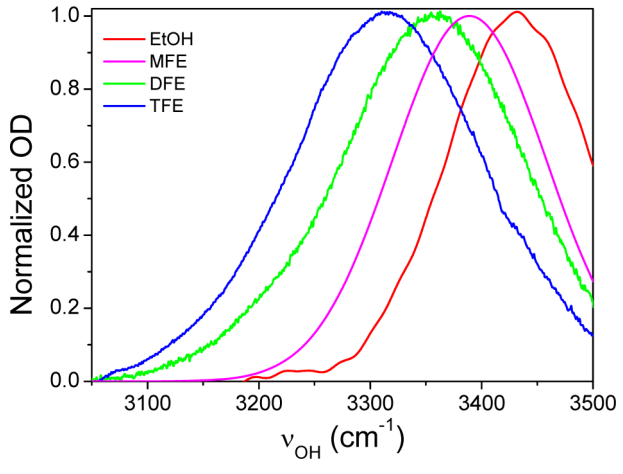

Figure 3. IR absorption bands of H-bonded complexes of fluoroethanols with the base DMSO in CCl_4 solvent. The frequencies of the maximum absorption ν_{OH} are summarized in Table 2. fwhm values of the IR absorption bands are 139, 153, 200, and 207 cm^{-1} for ethanol, monofluoroethanol, difluoroethanol, and trifluoroethanol, respectively.

Typical IR spectra of TFE forming 1:1 H-bonded complexes with the base DMSO in three representative solvents CCl_4, chlorobenzene, and dichloroethane (DCE) are shown in Figure 4. The solvent-induced shift in ν_{OH} is clearly apparent in the red-edge of the spectra and is about 64 cm^{-1} when moving from CCl_4 to DCE solvent. All the bands are separate and almost symmetrical at their top. The center of the IR absorption bands practically coincides with the frequency of the maximum frequency. As can be seen from the spectra in Figures 3 and 4, the H-association bands exhibit a simple spectral contour close in shape to a Gaussian curve and reflect 1:l complexation.

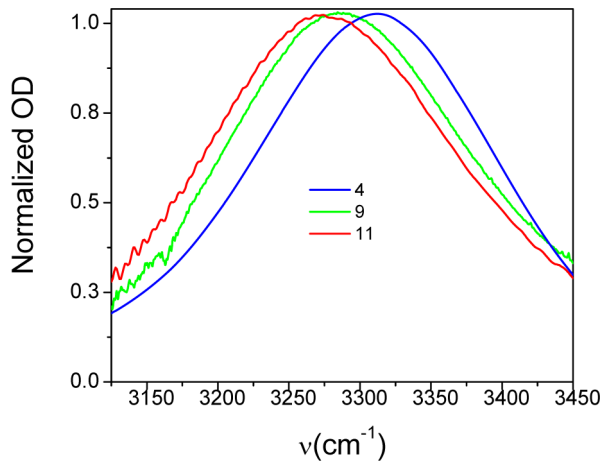

Figure 4. IR spectra for 1:1 H-bonded complexes of TFE with DMSO in CCl_4, chlorobenzene, and DCE solvents. The frequencies of the maximum absorption ν_{OH} are summarized in Table 2.

The experimental frequency ν_{OH} data are plotted versus the inverse of the solvent static dielectric constant ε in Figure 5 for the four substituted ethanol−DMSO complexes in both the nonpolar solvents 1−6 and the polar solvents 7−11 (cf. Tables 1 and 2). The solid and dashed lines are the linear correlations between ν_{OH} and $1/\varepsilon$ for nonpolar and polar solvents, respectively, to be discussed with the aid of our theory in section 4, where theoretically constructed curves will be compared to the data in Figure 5. Here we just stress certain key points evident from the experimental results in Figure 5.

A first general point concerning the H-bonded complexes is that, for a given solvent, the OH frequency is increasingly red-shifted with increasing fluorine substitution. A first general point concerning solvent effects is that the good correlation of the OH frequency with $1/\varepsilon$ for both nonpolar and polar solvents demonstrates that nonspecific dielectric interactions are indeed the main cause for the observed red-shift of ν_{OH} for this group of DMSO-complexed acids within these solvent sets. These interactions and their effects differ for the two types of solvents, as reflected both in the magnitude of ν_{OH} and in its variation with $1/\varepsilon$. For each alcohol, the slopes of the data for the nonpolar solvents are different from, and larger than, those for the polar solvents; this type of feature was first found and explained in refs 11 and 12.

The linear correlations were plotted for each of the two solvent groups separately (Figure 5). The intersection point of the extrapolated polar slope (dashed line) with the nonpolar

dx.doi.org/10.1021/jp509914w | J. Phys. Chem. B 2015, 119, 9278−9286

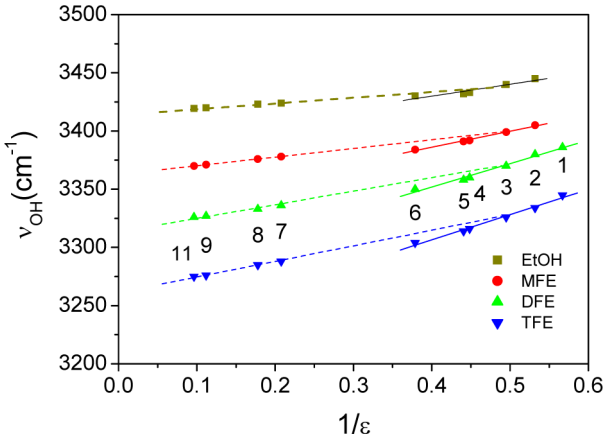

Figure 5. OH frequency ν_{OH} of the four DMSO-substituted ethanol H-bonded complexes versus the inverse of the solvent dielectric constant $1/\varepsilon$ for the nonpolar solvents (1–6) and for the polar solvents (7–9, 11). The solid and dashed lines are linear correlations for nonpolar and polar solvents, respectively (and are not theoretical predictions; see section 4). The intersection between the two correlation lines is at $\varepsilon = \varepsilon_\infty \approx 2$. The slopes of the linear correlations are summarized in Table 3. The inspiration to consider separate slopes for the nonpolar and polar solvents derives from the results presented in refs 11 and 12.

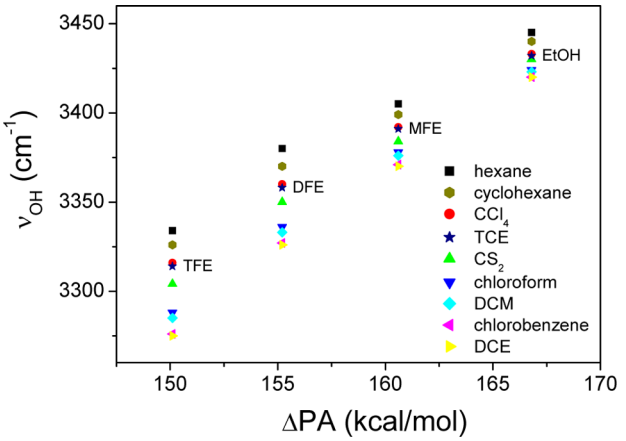

Figure 6. ν_{OH} for the four H-bonded alcohol–DMSO complexes in solution plotted versus the acidity measure involving the gas phase difference ΔPA of the proton affinity (PA): ΔPA = PA(conjugate base of the acid) − PA(complexing base). The acidity of the alcohol increases with decreasing ΔPA; since the complexing base DMSO is fixed, ΔPA reflects solely the PA (conjugate base of the acid) trend in the alcohols. The limited vertical range of ν_{OH} (for fixed ΔPA) associated with different dielectric solvents, compared to the typical magnitude of the ν_{OH} value itself, reflects the fact that solvent effects are much less effective than H-bond complex formation in red-shifting the frequency from the isolated alcohol ν_{OH} value (~3660 cm^{-1}).[11−13]

slope (full line) represents a zero polar solvent polarity limit where $\varepsilon = \varepsilon_\infty \approx 2$. The average value of ε_∞ for all the polar solvents used in our study is indeed equal to 2. Evidently, the effect of a nonpolar solvent is always larger than the effect of a polar solvent having the same dielectric constant as the nonpolar solvent. Below $\varepsilon \approx 2$, only nonpolar solvents exist by our definition, since there $\varepsilon = \varepsilon_\infty \approx n^2$. Theoretical curves close to the empirical ones in Figure 5 will be presented in section 4.

As discussed in more detail in section 4, the theory predicts[11] that the frequency red-shift increases with increasing acidity of the substituted alcohol acid partner in the complex. Figure 6 displays the experimental ν_{OH} for the four H-bonded complexes in solution plotted versus the acidity measure of the acid partner in the H-bonded complex. This is the gas phase difference ΔPA of the proton affinity (PA): ΔPA = PA(conjugate base of the acid) − PA(complexing base). With the fixed DMSO base, ΔPA decreases as the acidity of the alcohol increases, so that Figure 6 confirms the theory prediction mentioned above.

A further illustration of the experimental impact of ΔPA is displayed in Figure 7, indicating the increasing slope of ν_{OH} versus inverse solvent dielectric constant, for both solvent classes, with decreasing ΔPA.

In the next section, we turn to the theoretical perspective for all of the trends apparent in Figures 5–7.

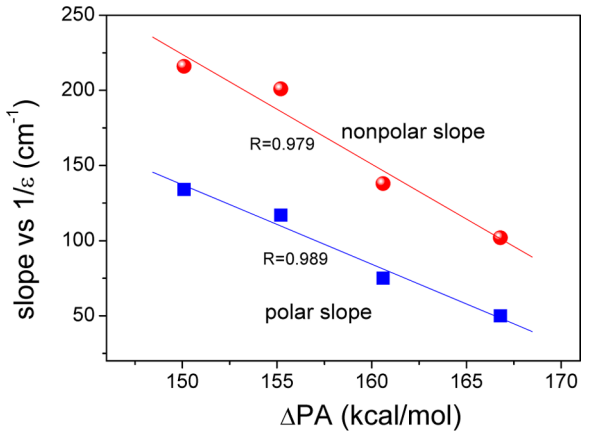

Figure 7. Slopes of Figure 5 ν_{OH} vs $1/\varepsilon$ plots for DMSO H-bonded fluoroethanols in polar and nonpolar solvents versus the proton affinity difference ΔPA. The linear correlations of Figure 5 listed in Table 3 are used to construct this plot.

4. DISCUSSION

In this section, we employ the theory developed in ref 11 to interpret the key features of the experimental results displayed in Figures 5 and 6. Here we just recap the essential aspects.

Important aspects of the theory include focus on an H-bonded complex itself dissolved in a solvent, a two Valence Bond (VB) state approach to the electronic structure involving a neutral state (N: AH···B) and an ionic state (I: $A^-\cdots HB^+$). This accounts for charge transfer (CT) within the H-bond complex, a solvation and or vibrational transition shift of population from that of the neutral VB state to the ionic one. Further features of the theory are quantization of the proton and H-bond coordinates of the complex and attention to nonequilibrium solvation issues for both the solvation and the Franck–Condon vibrational transitions. The theory emphasizes the overall importance of CT and acidity, both of which reflect the solvent-dependent electronic contribution of the ionic VB state. Further, both of these are coupled to the proton potential anharmonicity.

Evaluation of the theoretical expressions for the proton frequencies and their variations with solvent involved some electronic structure calculations, some vacuum molecular parameters, and some limited parametrization. As outlined in ref 11, parametrization was effected for a reference nonpolar solvent with $\varepsilon = \varepsilon_\infty = 2$. For the present family of fluorinated ethanol–DMSO complexes, the parameters for all complexes are assumed identical, except for a few parameters, such as

dx.doi.org/10.1021/jp509914w | J. Phys. Chem. B 2015, 119, 9278–9286

acidity ΔPA, that change with the added fluorine substitution of the acids; these are described in section 4.1. With the basic success of the theory already demonstrated for other acid systems,[11,12] this parametrization indicates which are the key OH frequency trends for this family. We discuss some further details when we discuss the slopes in the next section.

4.1. Frequency versus 1/ε Slopes. We begin with Figure 8, which presents again the experimental OH frequency results

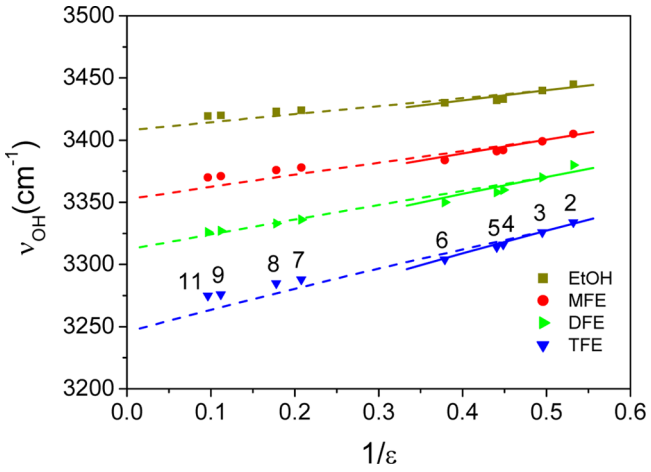

Figure 8. ν_{OH} of the four DMSO-substituted ethanol H-bonded complexes versus the inverse of the solvent dielectric constant $1/\varepsilon$ for the nonpolar (2–6) and polar (7–9, 11) solvents and the fits (lines) of ν_{OH} by theory. Perfluoroheptane (solvent 1) was not included in the correlation, because of the low solubility of ethanol and monofluoroethanol in this solvent. Lines are the theoretical results for the nonpolar (dashed lines) and polar (solid lines) solvent variation (in contrast to the empirical fits in Figure 5).

versus the inverse of the solvent dielectric constant; this figure also includes the theoretical predictions in contrast to the empirical linear correlations shown in Figure 5.

We expand on our brief remarks just given concerning the parametrization involved in the generation of Figure 8 theory curves (using the slope eqs 1 and 3 below). The ethanol–DMSO parameters are determined, as in ref 11, to give the correct nonpolar solvent slope and ν_{OH} magnitude for the reference $\varepsilon = \varepsilon_\infty = 2$ solvent. A difference from ref 11 is that, since ethanol–DMSO data for two additional nonpolar solvents (2 and 5 of Table 1) have become available, this parametrization protocol was repeated with the additional data. The only significant parameter change for the ethanol–DMSO complex from the prior results is an ∼20% increase in the ethanol–DMSO structure factor M_S, which is a measure of the H-bonded complex "size". The parameters for the other three fluorinated ethanol–DMSO complexes are taken to be identical to those of the ethanol–DMSO complex, except for ΔPA and those that determine the ground state dipole moment of the complex μ_{eq} and the equilibrium H-bond length Q_{eq}; as a consequence, μ_{eq} increases and Q_{eq} decreases on going from the ethanol to trifluoroethanol acid partners. It is important to note that we assume that the "size" of the complex is relatively unchanged within this fluorinated ethanol family of acids, and thus assume that M_S is identical for all of the complexes. In this way, the curves in Figure 8 for all the complexes in both the nonpolar and polar solvents are generated.

While the experiment–theory agreement in Figure 8 is not perfect, the reasonable agreement does illustrate that the variation of the key characteristics that define this family of complexes, i.e., the ΔPA, μ_{eq}, and Q_{eq} tendencies with flourine substitution, generates trends for the OH frequency that are consistent with those observed experimentally. Specifically, the magnitude of the polar and nonpolar slopes and their increase with increased substitution of the acids observed in Figure 5 and Table 3 are reasonably well reproduced by the theoretical curves of Figure 8.

Before proceeding to the discussion of the theory for the slopes, it is useful to first provide a perspective on the magnitude of the OH frequency and its relationship to the free energy G description of the theory. Figure 9 illustrates some of the relevant features. Figure 9a represents the effective proton potential in the H-bonded complex versus the OH stretch coordinate q, as composed of the strongly electronically diabatic VB neutral and ionic state free energies. ΔE is the free energy gap between the two VB states, which serves as a convenient measure of the asymmetry of the proton potential. Figure 9b illustrates the influence of increasing anharmonicity on the proton potential, tending toward increasing relative stabilization of the ionic pair form compared to the neutral pair form. This effect has a number of sources. The key solvent source, albeit usually of a much lesser effect than H-bonded complex sources, is an increasing dielectric constant, for both nonpolar and polar solvents. We illustrate the effect here via an important H-bonded complex source, the influence of increasing acidity of the acid member of the H-bonded complex, measured by the proton affinity difference ΔPA. The degree of charge transfer (which is related to ΔPA) could also have been used. Finally, in Figure 9c, we qualitatively illustrate the influence of the increasing anharmonicity illustrated in Figure 9b on the proton vibrational levels, which reduces their gap, thus red-shifting the OH frequency ν_{OH}.

We now turn to the theory for slopes of the OH frequency versus $1/\varepsilon$ plots in Figure 8. The slopes there (and in Figure 5) are clearly different for nonpolar and polar solvents. For the

Table 3. Slopes of ν_{OH} versus $1/\varepsilon$ Plots for DMSO H-Bonded Fluoroethanols in Polar and Nonpolar Solvents, Values of Proton Affinities PAs, the Proton Affinity Difference ΔPA, pK_a (Aqueous), and Taft Substituent Parameter σ* for the 1:1 H-Bonded Complexes of $CH_nF_{3-n}CH_2OH$ and DMSO

	slope[a] (cm^{-1}), nonpolar solvents	slope[a] (cm^{-1}), polar solvents	PA[22–24] (kcal/mol)	ΔPA[b] (kcal/mol)	pK_a[13,25] (aqueous)	σ*[c,13,25]
EtOH	102	50	370.8	166.8	15.9	−0.1
MFE	138	75	364.6	160.6	14.5	0.24
DFE	201	117	359.2	155.2	13.3	0.58
TFE	216	134	354.1	150.1	12.4	0.92

[a]Slopes of the lines used in Figure 5 for the linear correlations of the ν_{OH} vs $1/\varepsilon$ plots. [b]PA(DMSO) = 204.0 kcal/mol, ΔPA = PA − PA(DMSO). [c]σ* values are discussed in section 4.

dx.doi.org/10.1021/jp509914w | J. Phys. Chem. B 2015, 119, 9278–9286

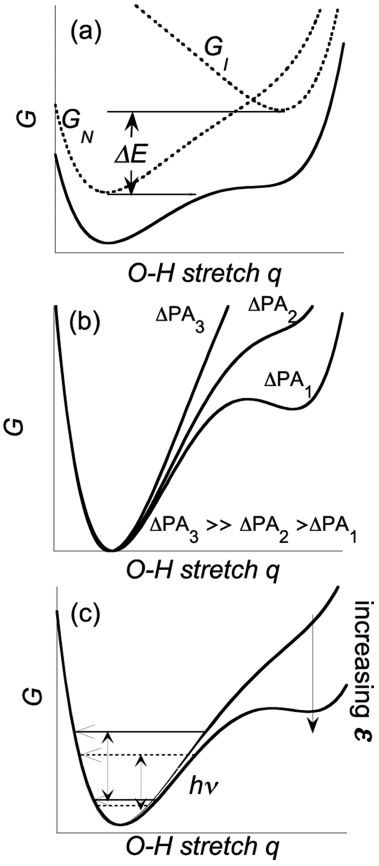

Figure 9. (a) Two VB state representations for the proton potential. G_N is the diabatic proton potential for the neutral H-bonded complex, and G_I is the diabatic proton potential for the ionic, proton-transferred complex. The abscissa is the OH stretch coordinate, i.e., the "proton" coordinate. ΔE is the free energy gap between the two VB states. Such a ΔE perspective has been extremely useful for understanding PT reactions in polar solvents.[26−28] (b) Schematic free energy proton potential G versus the proton stretch coordinate q for three ΔPA values, indicating the increasing anharmonicity and contribution of the ionic state with decreasing ΔPA, i.e., increasing acidity of the acid partner in the complex. (c) Schematic illustration of the proton vibrational energy levels for the two extreme ΔPA cases in part b. The influence of increasing anharmonicity on the vibrational levels, and thus the frequency ν_{OH}, is schematically indicated for the larger (solid lines) to smaller (dotted lines) ΔPA cases (from smaller to larger acidity of the H-complex acid partner). The H-bond coordinate Q, i.e., the O···O separation in the complex, is fixed for convenience.

former, as explained in refs 11 and 12, the only solvent polarization is the ultrarapid electronic variety, which can be assumed to equilibrate to the proton motion in the OH vibration and in the Franck−Condon vibrational transition. The predicted slope is[11]

$$\frac{d h\nu}{d(1/\varepsilon)} = M_s\{\langle M_2(q, Q)\rangle_1 - \langle M_2(q, Q)\rangle_0\} \quad (1)$$

where M_s is the structure factor inversely related to the complex's size and the braces enclose the difference in the excited and ground vibrational state quantum averages of M_2, the square of the electronic dipole moment operator evaluated in the ground electronic state of the complex

$$M_2(q, Q) \equiv \langle \hat{\mu}^2\rangle_{el} = \mu_N{}^2(q, Q)c_N{}^2(q, Q) + \mu_I{}^2(q, Q)c_I{}^2(q, Q) \quad (2)$$

This involves the dipole moments in, and the populations of, the neutral and ionic VB states. The former depend on the proton and H-bond length coordinates (q, Q), and the latter depend on those coordinates as well as the solvent dielectric ε_∞ constant, since the electronic structure of the complex is polarized (compared to the vacuum) by the solvent.

In polar solvents, there is equilibrium solvent electronic polarization but nonequilibrium solvent orientational polarization. Here the theory's predicted slope differs fundamentally from the nonpolar solvent slope above, and has the relatively simple analytic expression

$$\frac{d h\nu_{OH}}{d(1/\varepsilon)} \approx 2M_s[\langle\mu\rangle_{eq1} - \langle\mu\rangle_{eq0}]\langle\mu\rangle_{eq0} \quad (3)$$

Here $\langle\mu\rangle_{eq0}$ is the complex's ground vibrational state equilibrium dipole moment and the term in the square brackets is the difference in the expectation values of μ for the excited and ground proton stretch vibrational states, evaluated for the solvent's ground vibrational state equilibrium reaction field. Here it is to be understood that the electronic polarization contribution to the dielectric constant is held constant. Thus, in eq 1, ε reflects exclusively the solvent electronic polarization, while, in eq 3, it reflects exclusively the variation with the solvent nuclear orientation polarization.

The different slopes observed for nonpolar and polar solvents in Figures 8 and 5—with the former the larger of the two (cf. Table 3)—have their primary origins in the fact that the solvent is fully equilibrated in the former case but not in the latter case; the nonpolar solvent has a greater impact for a given change in the inverse dielectric constant. For the remainder of the present discussion, we focus on the more important polar solvent case, with theoretical slope eq 3.

The theory indicates that the slope of the ν_{OH} vs $1/\varepsilon$ plots is larger for the following:

1. Larger ground state dipole moment μ_{eq} of the complex, which induces greater coupling to the solvent in the ground vibrational state before the IR transition. This is borne out in Figures 5 and 8; recall that the dipole moment of the H-bonded complex increases on going from the ethanol to trifluoroethanol acid partners.
2. Larger excited/ground vibrational state difference of the dipole components of eqs 1 and 3, i.e., $\{\langle M_2\rangle_{eq1} - \langle M_2\rangle_{eq0}\}$ and $\{\langle\mu\rangle_{eq1} - \langle\mu\rangle_{eq0}\}$, respectively. With decreasing ΔPA in Figure 5 (see also Table 3), the gap ΔE is diminished, increasing both charge transfer and anharmonicity (Figure 9).
3. Smaller H-bonded complex size. With a larger structure factor M_s increasing the electrostatic interaction of the solvent with the solute and solvation energy increase. In the present study, M_s is taken to be the same for all the present complexes. Thus, this size effect is absent here.

4.2. Influence of the Alcohol Acidity. We have already stressed in several places above the importance of the acidity of the fluorinated alcohol series partner for the OH frequency and its variation with the solvent dielectric constant, most recently in item 2 just above in connection with the ν_{OH} versus $1/\varepsilon$ slopes. Here we give a more extended discussion, focused on the results in Figures 5, 6, 7, and 8.

dx.doi.org/10.1021/jp509914w | J. Phys. Chem. B 2015, 119, 9278−9286

Figure 6 displays the experimental trend that, for each solvent, the OH frequency ν_{OH} decreases with decreasing difference ΔPA in the gas phase proton affinities (PA) of the conjugate base of the alcohol acid and the fixed DMSO base, i.e., the increasing acidity of the fluorinated alcohol partner in the H-bonded complex (see Table 3). The influence of the solvent trend in Figure 6 is more clearly emphasized in Figure 7, which shows that the experimental slope of ν_{OH} versus the inverse of the solvent dielectric constant increases with increasing acidity. Figure 9 illustrates how the two VB construction affects the proton potential shape, and thus also the resulting ν_{OH}.

Figure 9 indicates the basic components of the influence of acidity from a theoretical perspective. Parts a and b of Figure 9 show how the electronically coupled two VB state representation in terms of the diabatic neutral (N: AH···B) and ionic (I: $A^-\cdots HB^+$) states influences the effective potential for the proton motion, its asymmetry (measured by the gap ΔE), and its resulting anharmonicity and thus ultimately the frequency ν_{OH}. Increasing acidity, i.e., diminishing ΔPA, reduces the gap ΔE, favoring the participation of the (proton-transferred) ionic state, i.e., charge transfer, and increasing anharmonicity and decreasing the OH frequency, illustrated in Figure 9c. This ΔPA influence is accentuated with increasing dielectric constant of the solvent (Figures 6 and 7) by increasing solvation of the ionic VB state, which reduces the gap ΔE, thus reinforcing the impact of the acidity. As we noted above, the solvation is more effective for the nonpolar solvents due to the instantaneous equilibration to the proton motion and the vibrational Franck–Condon transition lacking for the polar solvents where nonequilibrium solvation prevails; this accounts for the larger nonpolar solvent slope in Figure 7.

Finally, we can pursue the theme of the importance of ΔPA and alcohol acidity in another fashion by consideration of the Taft σ^* substituent effect parameter[15] of the fluorinated ethyl groups $CH_nF_{3-n}CH_2-$. Generally speaking, σ^* values here represent the overall substituent effect on the functional group (OH) as determined by measuring a property associated with the chemical reactivity of the functional group such as reaction rates or equilibrium constants. σ^* values often reflect both electronic and structural changes.

In fact, the linear correlation between σ^* and pK_a has already been demonstrated for this family of fluorinated ethanols, and in this particular case of the fluoroethanols, the changes are almost entirely electronic.[13,25] Figure 10 shows the plot of σ^* vs PA of the conjugate base of the fluoroethanols as well as for some related H- and fluoroalcohol systems. We thus find that σ^* also correlates with the proton affinity PA (the varying contribution of ΔPA for our H-bonded complexes), making this family of acids suitable for studying the effect of gradually modifying the PA of their conjugate base RO^-—when increasing the inductive effect of the R substituent. In the present H-bonded complex and solution context, the excellent correlation of σ^* with ΔPA found is helpful for highlighting the physical parameters which affect H-bonding interactions in solutions under conditions when the structure of the complex is little varied by either the solvent or the H-bonding interaction strength.

5. CONCLUDING REMARKS

We have presented infrared spectroscopic results for the OH vibrational frequency ν_{OH} for a series of hydrogen-bonded complexes of fluorinated ethanol acids (ethanol through trifluoroethanol) with dimethyl sulfoxide (DMSO) base in nonpolar and polar solvents with a focus on solvent and acidity effects. It is shown that ν_{OH} tends to decrease in a linear fashion with a decrease of the inverse of the solvent static dielectric constant $1/\varepsilon$. Strong linear correlations with ΔPA are found for both the frequency and its variation with $1/\varepsilon$. ΔPA is the difference in the gas phase proton affinity (PA) of the conjugate base of the alcoholic acid and the DMSO base and is a measure of the acidity of the alcoholic acid, which increases as ΔPA increases. A change in the measure of the acidity of the acid PA is not the exclusive consequence of the increased fluorine substitution of the acid. The complex dipole moment μ_{eq} increases and the equilibrium H-bond length Q_{eq} decreases on going from ethanol to trifluoroethanol. These μ_{eq} and Q_{eq} trends also correlate with acidity via ΔPA, such that they contribute to the ΔPA correlations in Figures 6 and 7. In addition, it is shown that ΔPA correlates linearly with the well-known Taft σ^* parameter for substituent effects. These solvent and acidity affects are well accounted for by our previously constructed theory. This success suggests that further development of the theory focused more specifically on acidity effects would be useful, and this is underway.

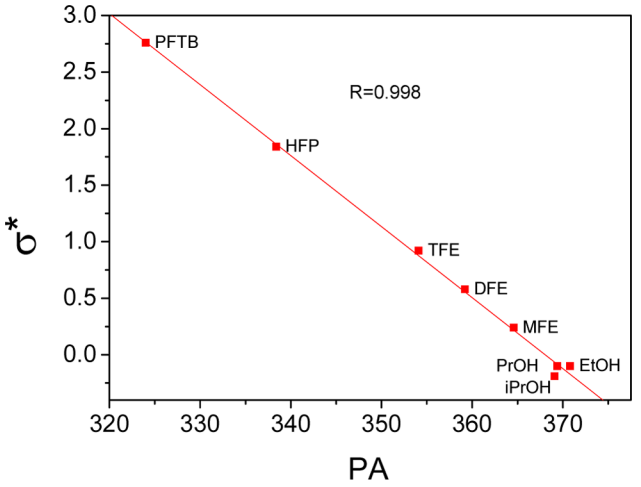

Figure 10. Linear σ^* of the R substituents versus PA plot for the fluoroethanols (ROH) listed in Table 3. Also plotted are 1,1,1,3,3,3-hexafluoro-2-propanol (HFP), perfluoro-*tert*-butyl alcohol (PFTB, propanol (PrOH), and isopropanol (iPrOH).

AUTHOR INFORMATION

Corresponding Authors

*E-mail address: James.Hynes@colorado.edu.

*E-mail address: epines@bgu.ac.il.

Notes

The authors declare no competing financial interest.

ACKNOWLEDGMENTS

This work was supported in part by Israel-USA Binational Science Foundation Grant No. 2006276 (E.P., J.T.H.) and by NSF grant CHE-1112564 (J.T.H.).

REFERENCES

(1) Pimentel, G. C.; McClellan, A. L. *The Hydrogen Bond*; W.H. Freeman: San Francisco, CA, 1960.

(2) Joesten, M. D.; Schaad, L. J. *Hydrogen Bonding*; Marcel Dekker, Inc.: New York, 1974.

(3) Jeffrey, G. A. *Introduction to Hydrogen Bonding*; Oxford University Press: Oxford, U.K., 1997.
(4) Grabowski, S. J. *Hydrogen Bonding: New Insights*; Springer: New York, 2006.
(5) Bell, R. P. *The Proton in Chemistry*, 2nd ed.; Chapman and Hall: London, 1973.
(6) van der Zwan, G.; Hynes, J. T. Dynamical polar solvent effects on solution reactions: A simple continuum model. *J. Chem. Phys.* **1982**, *76*, 2993−3001.
(7) Hynes, J. T.; Klinman, J. P.; Limbach, H.-H.; Schowen, R. L. *Hydrogen-Transfer Reactions*; Wiley-VCH Verlag GmbH & Co. KgaA Weinheim: Weinheim, Germany, 2007.
(8) Elsaesser, H. Bakker, T. *Ultrafast hydrogen bonding dynamics and proton transfer processes in the condensed phase*; Kluwer Academic Publishers: Dordrecht, The Netherlands, 2002.
(9) Lorente, P.; Shenderovich, I. G.; Golubev, N. S.; Denisov, G. S.; Buntkowsky, G.; Limbach, H.-H. $^{1}H/^{15}N$ NMR Chemical Shielding, Dipolar $^{15}N,^{2}H$ Coupling and Hydrogen Bond Geometry Correlations in a Novel Series of Hydrogen-Bonded Acid-Base Complexes of Collidine with Carboxylic Acids. *Magn. Reson. Chem.* **2001**, *39*, S18−S29.
(10) Magnes, B.-Z.; Pines, D.; Strashnikova, N.; Pines, E. Hydrogen-bonding Interactions of Photoacids: Correlation of Optical Solvatochromism with IR Absorption Spectra. *Solid State Ionics* **2004**, *168*, 225−233.
(11) Kiefer, P. M.; Pines, E.; Pines, D.; Hynes, J. T. Solvent-Induced Red-Shifts for the Proton Stretch Vibrational Frequency in a Hydrogen-Bonded Complex. 1. A Valence Bond-Based Theoretical Approach. *J. Phys. Chem. B* **2014**, *118*, 8330−8351.
(12) Keinan, S.; Pines, D.; Kiefer, P. M.; Hynes, J. T.; Pines, E. Solvent-Induced O-H Vibration Red-Shifts of Oxygen-Acids in Hydrogen-Bonded O-H···Base Complexes. *J. Phys. Chem. B* **2014**, DOI: 10.1021/jp502553r.
(13) Schrems, O.; Oberhoffer, H. M.; Luck, W. A. P. Hydrogen bonding in low-temperature matrices. I: Proton donor abilities of fluoroalcohols —— Comparative Infrared Studies of ROH···O(CH3)-2 Complex Formation in the Gas Phase, in CCl_4 Solution, and in Solid Argon. *J. Phys. Chem.* **1984**, *88*, 4335−4342.
(14) Heger, M.; Schargez, T.; Suhm, M. A. From Hydrogen Bond Donor to Acceptor: the Effect of Ethanol Fluorination on the first Solvating Water Molecule. *Phys. Chem. Chem. Phys.* **2013**, *15*, 16065−16073.
(15) Taft, R. W. Polar and Steric Substituent Constants for Aliphatic and o-Benzoate Groups from Rates of Esterification and Hydrolysis of Esters. *J. Am. Chem. Soc.* **1952**, *74*, 3120−3128.
(16) Reichardt, C. *Solvents and Solvent Effects in Organic Chemistry*; Wiley-VCH: Weinheim, Germany, 1988.
(17) Kamlet, M. J.; Gal, J.-F.; Maria, P.-C.; Taft, R. W. Linear Solvation Energy Relationships. Part 32. A Co-ordinate Covalency Parameter, ξ, which, in Combination with the Hydrogen Bond Acceptor Basicity Parameter, β, Permits Correlation of Many Properties of Neutral Oxygen and Nitrogen Bases (Including Aqueous pK_a). *J. Chem. Soc., Perkin Trans. 2* **1985**, 1583−1589.
(18) Marcus, Y. The Properties of Organic Liquids that are Relevant to their Use as Solvating Solvents. *Chem. Soc. Rev.* **1993**, *22*, 409−416.
(19) Kamlet, M. J.; Abboud, J. L. M.; Abraham, M. H.; Taft, R. W. Linear Solvation Energy Relationships 0.23. a Comprehensive Collection of the Solvatochromic Parameters, Pi-Star, Alpha and Beta, and Some Methods for Simplifying the Generalized Solvatochromic Equation. *J. Org. Chem.* **1983**, *48*, 2877−2887.
(20) Brady, J. W.; Carr, P. Perfluorinated Solvents as Nonpolar Test Systems for Generalized Models of Solvatochromic Measures of Solvent Strength. *Anal. Chem.* **1982**, *54*, 1751−1757.
(21) Hu, Y. J.; Fu, H. B.; Bernstein, E. R. Infrared Plus Vacuum Ultraviolet Spectroscopy of Neutral and Ionic Ethanol Monomers and Clusters. *J. Chem. Phys.* **2006**, *125*, 154305.
(22) NIST Chemistry WebBook, http://webbook.nist.gov.
(23) Hunter, E. P. L.; Lias, S. G. Evaluated Gas Phase Basicities and Proton Affinities of Molecules: An Update. *J. Phys. Chem. Ref. Data* **1998**, *27*, 413.
(24) Bartmess, J. E.; Scott, J. A.; McIver, R. T., Jr. The Gas Phase Acidity Scale from Methanol to Phenol. *J. Am. Chem. Soc.* **1979**, *101*, 6046−6056.
(25) Sherry, A. D.; Purcell, K. F. Linear Enthalpy-Spectral Shift Correlations for 2,2,2- Trifluoroethanol. *J. Phys. Chem.* **1970**, *74*, 3535−3543.
(26) Kiefer, P. M.; Hynes, J. T. Proton Transfer Reactions in a Polar Environment. In *Hydrogen-Transfer Reactions*; Hynes, J. T., Klinman, J. P., Limbach, H.-H., Schowen, R. L., Eds.; Wiley-VCH Verlag GmbH &Co. KgaA Weinheim: Weinheim, Germany, 2007; Vol. *1*, pp 307−348.
(27) Ando, K.; Hynes, J. T. Molecular Mechanism of HCl Acid Ionization in Water: ab initio Potential Energy Surfaces and Monte Carlo Simulations. *J. Phys. Chem. B* **1997**, *101*, 10464−10478.
(28) Ando, K.; Hynes, J. T. Molecular Mechanism of HF Acid Ionization in Water: An Electronic Structure−Monte Carlo Study. *J. Phys. Chem. A* **1999**, *103*, 10398−10408.